Patterning of Small Particles by a Surfactant-Enhanced Marangoni-Bénard Instability

Van X. Nguyen
Department of Chemical Engineering, Johns Hopkins University, Baltimore, Maryland 21218

Kathleen J. Stebe
Department of Chemical Engineering, Materials Science & Engineering, and Biomedical Engineering, Johns Hopkins University, Baltimore, Maryland 21218

(Received 16 August 2001; published 3 April 2002)

Evaporating drops provide a means of organizing particles suspended within them. Here, the manner in which surfactants alter these patterns is studied as a function of the surface state of an insoluble monolayer at the drop interface. The surface state is visualized throughout the drop evolution using fluorescence microscopy. A regime of surfactant coverage is identified that creates conditions that enhance the Marangoni-Bénard instability. This result was not anticipated in prior studies, in which surfactants are predicted to prevent this instability. These data demonstrate that, by tuning the liquid-gas boundary condition, the patterns formed from an evaporating drop can be controlled.

DOI: 10.1103/PhysRevLett.88.164501 PACS numbers: 47.54.+r, 47.20.Dr, 47.20.Ma, 82.70.Uv

When a drop containing finely divided particles evaporates, the particles act as tracers and are deposited in well defined macroscopic patterns on the substrate by the flow field. Interactions among the particles can be exploited to create local order. This phenomenon has been used as a means of organizing suspended particles with dimensions ranging from nanometers to micrometers [1–4]. Patterning of nanoparticles is an area of emerging interest in nanotechnology applications such as sensors and photonic devices [5,6]. Two of the patterns reported have been associated closely with flow fields within the drop. The first is a "coffee ring" pattern [1,2,7–10], formed when the contact line of the drop on the solid substrate becomes pinned by the local roughness created by the particles entrapped there. As the drop evaporates, solvent flows toward the contact ring, carrying suspended particles with it. Once the solvent has evaporated, a ring of particles is left as residue. The second pattern is spatially periodic and is formed by Bénard convection [3,4]. As the solvent evaporates, the drop cools at the interface, establishing a temperature gradient as a function of depth. Small perturbations in the surface temperature create gradients in the surface tension. The interface contracts toward the high tension regions, establishing a temperature-driven Marangoni flow that pulls hot fluid to the interface from below the warm regions, reinforcing the instability. Associated with this instability is a characteristic wavelength that agrees well with the dimensions of the periodic flow patterns or Bénard cells. This length scale also characterizes the patterns of particles deposited by the flow.

For surfactant-free systems, conditions that lead to Bénard cells are well established [11,12]. The Marangoni number, $B = [-\frac{\partial\gamma}{\partial T}\frac{\beta d^2}{\kappa\eta}]$, is defined as the ratio of the time scale for the temperature perturbation to propagate across the film, $\frac{d^2}{\kappa}$, where κ is the thermal diffusivity and d is the depth of the fluid, to the time scale for the Marangoni flow to establish itself, $[-\frac{\partial\gamma}{\partial T}\frac{\beta}{\eta}]^{-1}$, where $\frac{\partial\gamma}{\partial T}$ is the derivative of the surface tension γ with respect to temperature T, β is the base state temperature gradient established by the evaporative flux, and η is the viscosity. Critical Marangoni numbers and wavelengths are well established for liquid films in a planar geometry.

Our interest concerns the role of surfactants in this process. Specifically, how do surfactants alter the patterns formed as a drop evaporates? Surfactants adsorb on interfaces and reduce the surface tension. Small perturbations in the surface concentration, Γ, create surface tension gradients given by $\frac{\partial\gamma}{\partial\Gamma}\nabla_s\Gamma$, where ∇_s is the surface gradient operator. Because these compositional Marangoni stresses oppose the motion which creates them, surfactants have been predicted and demonstrated experimentally to prevent Bénard flows [13,14]. However, patterns which appear to be created by Bénard cells have been reported to form after the evaporation of surfactant-laden drops containing microspheres [2]. Our aim is to understand how surfactants can create conditions which favor the occurrence of Bénard cells.

Surfactants can arrange in a series of surface states: the surface gaseous state (G) consists of surfactant molecules at an area per molecule large enough that the surfactant chains barely interact; the surface liquid expanded state (LE) consists of surfactants with tails oriented out of the interface in a disordered state; liquid condensed states (LC) consist of surfactants with highly ordered chains [15]. We report experiments performed on an evaporating drop as a function of the surface state of an insoluble monolayer of pentadecanoic acid (PDA). The state of the surfactant on the drop interface is visualized as the drop evaporates using fluorescence microscopy.

Drops of pH 2.0, HCl suspensions containing 0.01% solid w/v amidine- or sulfate-functionalized microspheres (Interfacial Dynamics Corp., 0.8 μm diameter) are

studied. These particles are strongly wet by water. They do not associate with the monolayer but are convected by the flow within the drop. A pendant drop is formed at the tip of a Teflon capillary. A monolayer of PDA (Fluka) is spread from ethanol onto the pendant drop surface using a 1 μL syringe. After the ethanol has evaporated, the surface tension is measured by comparing the digitized drop contour to shapes obtained from numerical solutions of the Young-Laplace equation [16]. The drop is then deposited on an octadecyltrichlorosilane-modified silicon dioxide substrate on which purified water forms a static advancing contact angle of $50 \pm 3°$. The drop forms a spherical cap with a pinned contact line. The silhouette of the evaporating sessile drop is recorded as a function of time, allowing the mass flux to be estimated. The PDA is doped with a fluorescent probe, 4-hexadecylamino-7-nitrobenez-2-oxa-1,3-diazole, NBD-HDA (Molecular Probes, Inc.), at no more than 1 mole %, allowing the surface phase of the surfactant to be imaged during the evaporation process. The relative humidity is maintained at 50% at a temperature of 23 ± 0.5 °C. The deposited drop volumes ranged from 6.5 to 8.4 μL, averaging 7.4 ± 0.5 μL. The mass flux remains fixed at roughly 2×10^{-4} $\frac{\text{kg}}{\text{m}^2\text{s}}$ for the first 30 min and agrees well with a diffusion controlled flux across the vapor space for a spherical cap. The mass flux does not vary with surfactant coverage, indicating that the interface does not exert a controlling role over evaporation for drops of this curvature.

An isotherm of the surface pressure (π) as a function of area per molecule (A) for PDA is reported in Fig. 1 with the regions corresponding to the various surface phases indicated. The G-LE [17] and LE-LC [15] phase transitions are first order. The fluorescence images of each of the single phase and coexistence regions are also shown. These images agree well with those reported previously in the presence of the probe [18] and with images obtained by Brewster angle microscopy [19]. The contrast provided by NBD-HDA arises because the probe is quenched in contact with water and fluoresces when shielded from water by hydrocarbon moieties. In the G phase, the probe is quenched. In the LE state, the probe is sequestered in the disordered hydrocarbon chains, permitting it to fluoresce. The order among the hydrocarbon chains in the LC state forces the probe out of the LC domains, causing this state to appear dark. Therefore, in G-LE coexistence, G domains are dark in a bright LE phase. In the LE state, the interface is uniformly bright. In LE-LC coexistence, the LC domains are dark on the bright LE background. When the interface is completely in the LC state, the interface is dark. For surface pressures above the equilibrium spreading pressure of the dye (~ 12 $\frac{\text{mN}}{\text{m}}$), small crystals of the dye form, appearing as bright speckles on the interface. These images provide a map for the surface state of the surfactant on the evaporating drop.

For drops deposited with surfactant-free interfaces, the outward flow to the contact ring causes the particles to form a coffee ring. Similar results are obtained for drops with interfaces in G-LE coexistence and in the LE state. Faint coffee rings also form in the LC state, although particles deposit nearly uniformly beneath the drop, indicating a weakened outward flow. For drops that are initially in LE-LC coexistence, the particles form a periodic network of roughly hexagonal shapes that are the signature of Bénard cells.

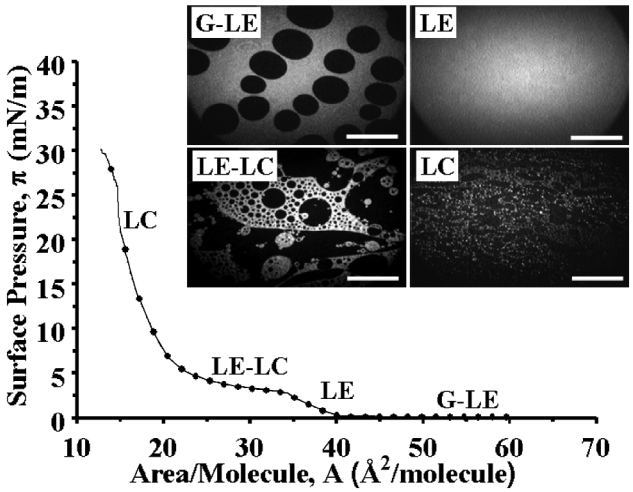

FIG. 1. Isotherm of PDA containing 1 mole % NBD-HDA with fluorescence images obtained on a Langmuir trough at 19.8 °C on a pH 2, HCl subphase at a compression rate of 0.832 Å^2/(moecule minute). Scale is 500 μm.

Typical results for the LE-LC state are reported in Fig. 2. Fluorescence images (Fig. 2a) confirm that the interface is in LE-LC coexistence. As the drop evaporates, the interface remains in coexistence. The microspheres begin to move, creating periodic hexagonal flow cells visible by reflected-light microscopy. The particles are deposited by the flow on the substrate, leaving a final pattern of particles in a connected network of polygons when evaporation is complete (Fig. 2b). Similar results are obtained with either sulfate-functionalized (shown) or amidine-functionalized microspheres. In Fig. 3, a drop with an interface initially in the LE state is deposited and forms a coffee ring as it evaporates. The drop then depins, hops (upwards and to the right in the figure), and evaporates at its new position. The interface is still in the LE state, and a new coffee ring pattern develops. Finally, this drop depins and hops again, contracting the drop interface and driving the monolayer into LE-LC coexistence. Only then does Bénard convection set in, and the particles deposit in the characteristic pattern (Fig. 3b). These results show that Bénard convection is present when the interface is in LE-LC coexistence, even though the interfacial concentration of surfactant is significant. This is contrary to what one would expect based on the prior work in the literature. There are two reasons that interfaces in LE-LC coexistence create conditions that favor Bénard convection:

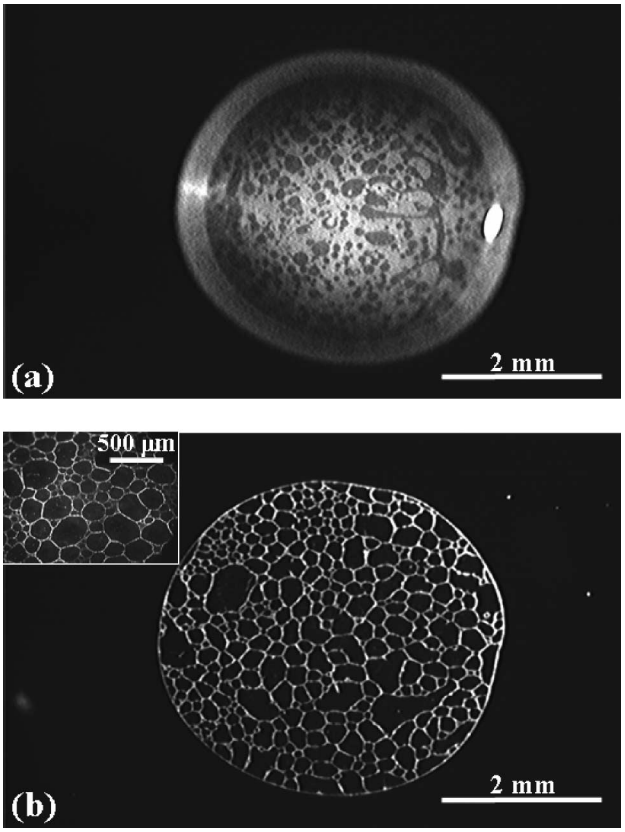

FIG. 2. (a) Fluorescence microscopy image of the sessile drop interface in the LE-LC coexistence. Note: the drop apex is in the focal plane, not the contact line. (b) Reflected-light microscopy image of the connected polygonal network formed by particles left as residue after the drop evaporates. In the bright regions, particles have accumulated to form a ridgelike structure. Dark regions are nearly free of particles.

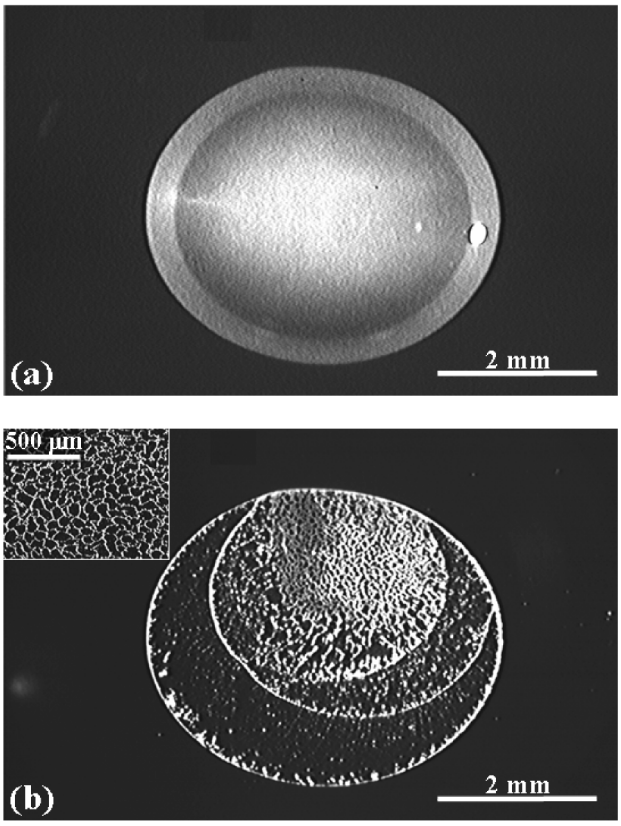

FIG. 3. (a) Fluorescence microscopy image of the interface of a drop initially in the LE state. (b) Reflected-light microscopy image of patterns left as residue after evaporation is complete. Inset: a close-up of the pattern formed in the region of the drop that was in LE-LC coexistence.

(i) In the LE-LC coexistence regime, compositional Marangoni stresses are weak.—For highly purified PDA, compositional Marangoni stresses are strictly zero, since, for first order phase transitions, $\frac{\partial \pi}{\partial A}|_T = \Gamma^2 \frac{\partial \gamma}{\partial \Gamma}|_T = 0$. (In our isotherm, there is a slight upward slope in this region, which is caused by trace contaminants in the PDA sample [20]. Even so, the slope of the coexistence region is far less than the single phase regions, and compositional Marangoni stresses are weak.) This also occurs in G-LE coexistence, which did not exhibit Bénard convection. Therefore, this weakened coupling between surface tension and surface concentration alone cannot explain why Bénard convection is limited to LE-LC coexistence.

(ii) In the LE-LC coexistence regime, temperature-driven Marangoni stresses are strong.—This effect strongly favors the occurrence of Bénard convection. For surfactants undergoing an LE-LC phase transition, the hydrocarbon chains become highly ordered with a small change in area per molecule, ΔA. Because the transition is first order, $\Delta S = \frac{\partial \gamma}{\partial T}|_{\mu_{\mathrm{LE}} = \mu_{\mathrm{LC}}} \Delta A$, where μ_{LE} and μ_{LC} are the chemical potential for the liquid expanded and liquid condensed phases, respectively. The strong change in entropy over the small area increment requires that the derivative $\frac{\partial \gamma}{\partial T}$ in coexistence be large. For clean water, $\frac{\partial \gamma_o}{\partial T} = -0.15 \ \frac{\mathrm{mN}}{\mathrm{m\,K}}$ [21]; for PDA in the G-LE state, $\frac{\partial \gamma}{\partial T} = -0.15 \ \frac{\mathrm{mN}}{\mathrm{m\,K}}$ [17], while for PDA in the LE-LC state, $\frac{\partial \gamma}{\partial T} = -1.29 \ \frac{\mathrm{mN}}{\mathrm{m\,K}}$ [15]. Thus, in LE-LC coexistence, the driving Marangoni stress for a given temperature fluctuation is enhanced by an order of magnitude.

In order to maintain a pinned contact line, the outward flow persists, and the coffee ring forms even in the presence of Bénard flow. The latter flow is dominant. In our experiments, the characteristic velocity for the Bénard flow $U_B \approx \frac{\partial \gamma}{\partial T} \frac{\beta d}{\eta} = 0.3 \ \frac{\mathrm{m}}{\mathrm{s}}$, while the characteristic velocity to create the coffee ring (CR) can be estimated [7] to be $U_{\mathrm{CR}} \approx 2 \times 10^{-7} \ \frac{\mathrm{m}}{\mathrm{s}}$.

It is interesting to consider the results of Deegan, who reported the formation of periodic patterns for evaporating drops containing microspheres in aqueous solutions of sodium dodecyl sulfate (SDS) [2]. SDS does not form a condensed surface state because of electrostatic repulsion among its headgroups. However, the hydrolysis product of SDS, dodecanol, does, as do mixtures of SDS and dodecanol [22,23]. Dodecanol spontaneously forms in SDS solutions and is far more surface active

than SDS itself [24], so interfaces of SDS solutions are typically enriched in dodecanol. Therefore, it is probable that the patterns were made by Bénard cells driven by the preferential adsorption of dodecanol which formed coexisting LE-LC states at the drop interface.

Marangoni-Bénard convection rarely occurs in aqueous systems. Because of the high surface tension of water, the interface is susceptible to adsorption of trace surface active impurities that can stabilize the interface. Rather, Bénard cells in aqueous systems are typically created by Rayleigh-Bénard convection, driven by adverse density gradients created by heating a fluid from below [25]. A linear stability analysis for Rayleigh-Bénard flow in a planar geometry reveals a critical Rayleigh number, $Ra = \frac{g\zeta\beta d^4}{\kappa\nu}$, at which convection occurs, where g is the gravitational acceleration, ζ is the coefficient of volume expansion, and ν is the kinematic viscosity. In our system, $Ra = 0.09$, orders of magnitude lower than the critical value $Ra_{\text{crit}} = 1108$ [26], confirming that density gradients are too weak to drive the observed flow.

The length scale of the features created by the deposited microspheres shown in the inset to Fig. 2b range from 200 to 250 μm. This corresponds well to the characteristic wavelength, λ, predicted for Bénard cells, where $\lambda = \frac{2\pi d}{\alpha}$ and α is the dimensionless wave number, related to the Marangoni number, $B = 8\alpha^2$, for large α [11]. In our case, $B = 650$ and $\lambda = 216$ μm (based on $\beta = 7.55\ \frac{\text{K}}{\text{cm}}$, $d = 0.031$ cm (the average drop height), $\eta = 0.01\ \frac{\text{g}}{\text{cm s}}$, $\kappa = 1.44 \times 10^{-3}\ \frac{\text{cm}^2}{\text{s}}$, and $\frac{\partial\gamma}{\partial T} = 1.29\ \frac{\text{mN}}{\text{m K}}$).

In conclusion, these experiments have revealed a regime in which surfactants create conditions that favor the occurrence of Bénard convection driven by thermal Marangoni stresses, which otherwise do not occur in aqueous systems. These results are of particular interest in systems where proteins or other biologically based materials are to be assembled. In these systems, aqueous depositions are favored in order to prevent conformational changes of the biologically active molecules [27].

We gratefully acknowledge support from NASA's Office of Biological and Physical Research (Grant No. NAG3-1923 from NASA Glenn Research Center) and by NASA's Graduate Student Researchers Program (Grant No. GNT5-50268).

[1] R. Deegan, O. Bakajin, T. F. Dupont, G. Huber, S. R. Nagel, and T. A. Witten, Nature (London) **389**, 827 (1997).
[2] R. D. Deegan, Phys. Rev. E **61**, 475 (2000).
[3] M. Maillard, L. Motte, and M. P. Pileni, Adv. Mater. **13**, 200 (2001).
[4] H. T. Wang, Z. B. Wang, L. M. Huang, A. Mitra, and Y. S. Yan, Langmuir **17**, 2572 (2001).
[5] C. B. Murray, C. R. Kagan, and M. G. Bawendi, Annu. Rev. Mater. Sci. **30**, 545 (2000).
[6] P. Alivisatos, Pure Appl. Chem. **72**, 3 (2000).
[7] R. Deegan, O. Bakajin, T. F. Dupont, G. Huber, S. R. Nagel, and T. A. Witten, Phys. Rev. E **62**, 756 (2000).
[8] E. Adachi, A. S. Dimitrov, and K. Nagayama, Langmuir **11**, 1057 (1995).
[9] F. Parisse and C. Allain, Langmuir **13**, 3598 (1997).
[10] K. Uno, K. Hayashi, T. Hayashi, K. Ito, and H. Kitano, Colloid Polym. Sci. **276**, 810 (1998).
[11] J. R. A. Pearson, J. Fluid Mech. **4**, 489 (1958).
[12] D. A. Nield, J. Fluid Mech. **19**, 341 (1964).
[13] J. C. Berg and A. Acrivos, Chem. Eng. Sci. **20**, 737 (1965).
[14] J. C. Berg, A. Acrivos, and M. Boudart, Adv. Chem. Eng. **6**, 61 (1966).
[15] S. Akamatsu and F. Rondelez, J. Phys. II (France) **1**, 1309 (1991).
[16] R. N. Pan, J. Green, and C. Maldarelli, J. Colloid Interface Sci. **205**, 213 (1998).
[17] N. R. Pallas and B. A. Pethica, J. Chem. Soc. Faraday Trans. 1 **83**, 585 (1987).
[18] B. G. Moore, C. M. Knobler, S. Akamatsu, and F. Rondelez, J. Phys. Chem. **94**, 4588 (1990).
[19] D. Honig, G. A. Overbeck, and D. Mobius, Adv. Mater. **4**, 419 (1992).
[20] N. R. Pallas and B. A. Pethica, Langmuir **1**, 509 (1985).
[21] *Lange's Handbook of Chemistry,* edited by J. A. Dean (McGraw-Hill Book Company, New York, 1985).
[22] B. D. Casson and C. D. Bain, J. Phys. Chem. B **102**, 7434 (1998).
[23] V. M. Fainerman, D. Vollhardt, and G. Emrich, J. Phys. Chem. B **105**, 4324 (2001).
[24] K. J. Mysels, Langmuir **2**, 423 (1986).
[25] W. G. Spangenberg and W. R. Rowland, Phys. Fluids **4**, 743 (1961).
[26] A. R. Low, Proc. R. Soc. London A **125**, 180 (1929).
[27] W. Kauzmann, Adv. Protein. Chem. **14**, 1 (1959).